Electrochemical Synthesis of Mesoporous Au-Cu Alloy Films with Vertically Oriented Mesochannels Using Block Copolymer Micelles

Asep Sugih Nugraha[1,2,3], Victor Malgras*[2], Muhammad Iqbal[2,3], Bo Jiang[2], Cuiling Li[2], Yoshio Bando[2,4], Abdulmohsen Alshehri[5], Jeonghun Kim[1,6], Yusuke Yamauchi[1,6,7]* and Toru Asahi[3]*

1 College of Chemistry and Molecular Engineering, Qingdao University of Science and Technology, Qingdao 266042, China

2 International Center for Materials Nanoarchitectonics (WPI-MANA) & International Center for Young Scientists (ICYS), National Institute for Materials Science (NIMS), 1-1 Namiki, Tsukuba, Ibaraki 305-0044, Japan

3 Faculty of Science and Engineering, Waseda University, 3-4-1 Okubo, Shinjuku, Tokyo 169-8555, Japan.

4 Australian Institute for Innovative Materials (AIIM), University of Wollongong, Squires Way, North Wollongong, New South Wales 2500, Australia

5 Department of Chemistry, King Abdulaziz University, P.O. Box 80203, Jeddah 21589, Saudi Arabia

6 School of Chemical Engineering & Australian Institute for Bioengineering and Nanotechnology (AIBN), The University of Queensland, Brisbane, QLD 4072, Australia

7 Department of Plant & Environmental New Resources, Kyung Hee University, 1732 Deogyeong-daero, Giheunggu, Yongin-si, Gyeonggi-do 446-701, South Korea

E-mails: MALGRAS.Victor@nims.go.jp; y.yamauchi@uq.edu.au; tasahi@waseda.jp

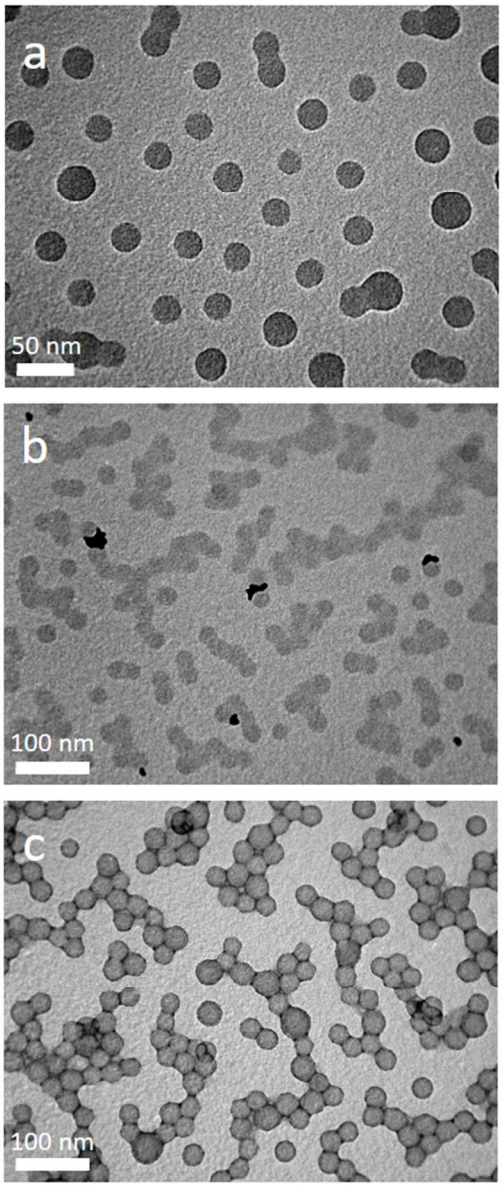

Figure S1 TEM images of polymeric micelles with various Au:Cu molar ratios ((a) 100:0, (b) 25:75, and (c) 0:100).

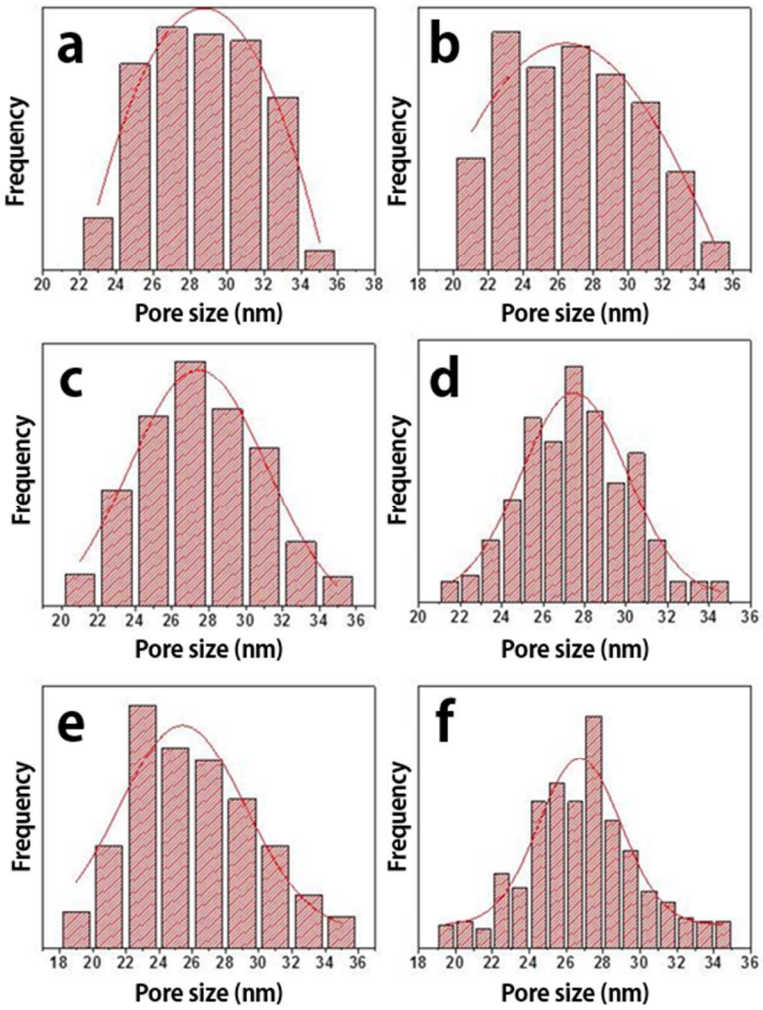

Figure S2 Pore size distribution of the mesoporous (a) Au_{100}, (b) $Au_{94}Cu_6$, (c) $Au_{87}Cu_{13}$, (d) $Au_{78}Cu_{22}$, (e) $Au_{49}Cu_{51}$, and (f) $Au_{41}Cu_{59}$ films.

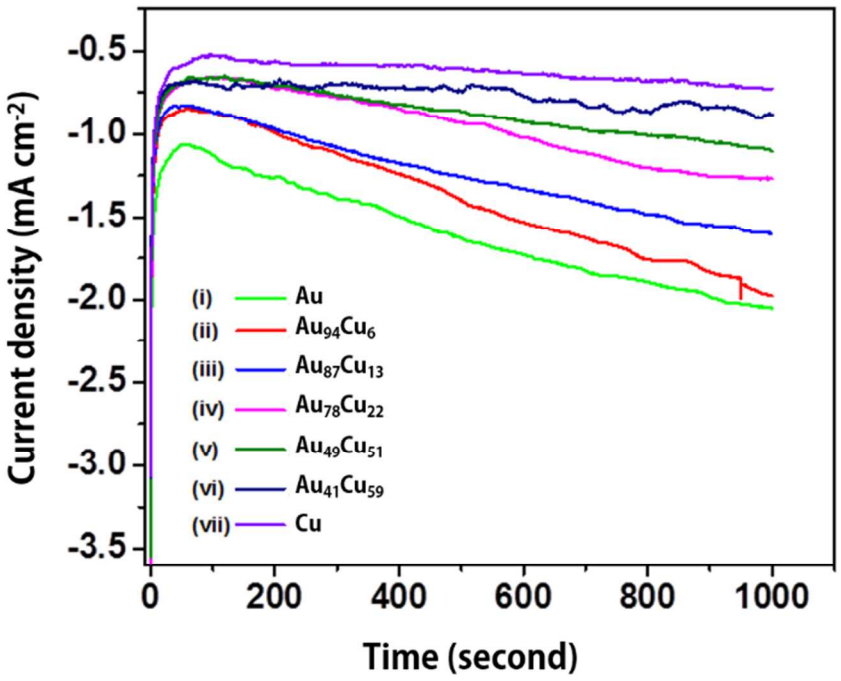

Figure S3 Amperometric plots for the deposition of mesoporous Au-Cu films with different compositions. Each process is carried out at room temperature at -0.5 V (*vs.* Ag/AgCl) for 1000 s. The current density was normalized by the geometrical electrode area.

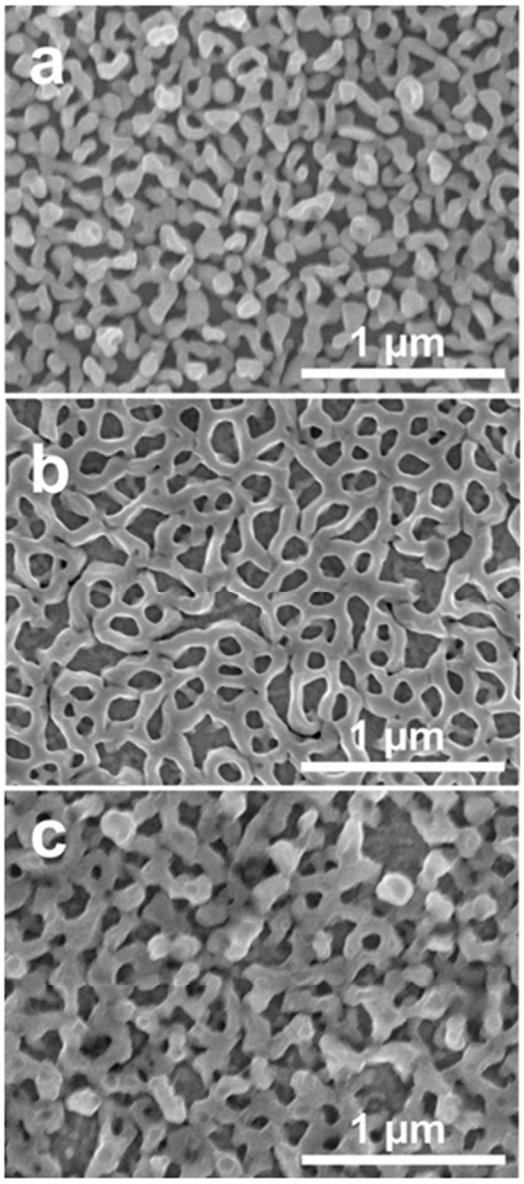

Figure S4 Typical SEM images of the obtained Cu films for 1000 s deposition and at various deposition potentials of (a) -0.5 V, (b) -0.4 V, (c) -0.35 V.

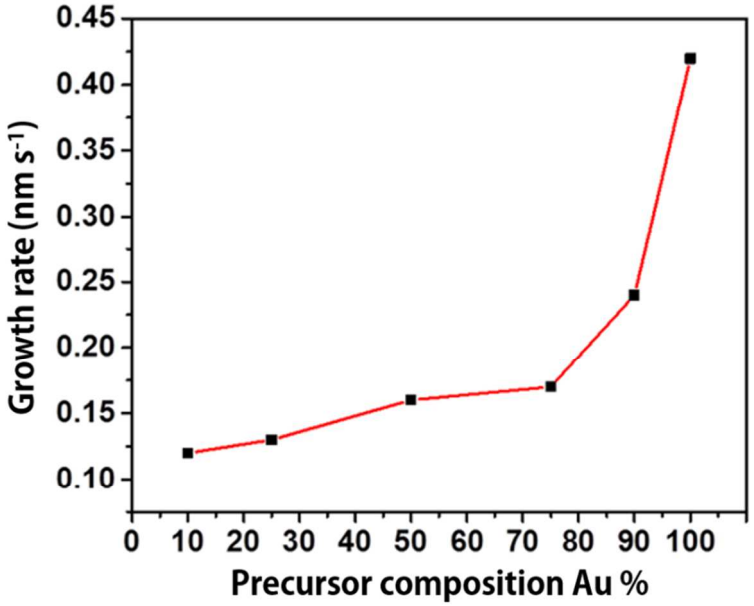

Figure S5 Relationship between film growth rate and precursor composition.

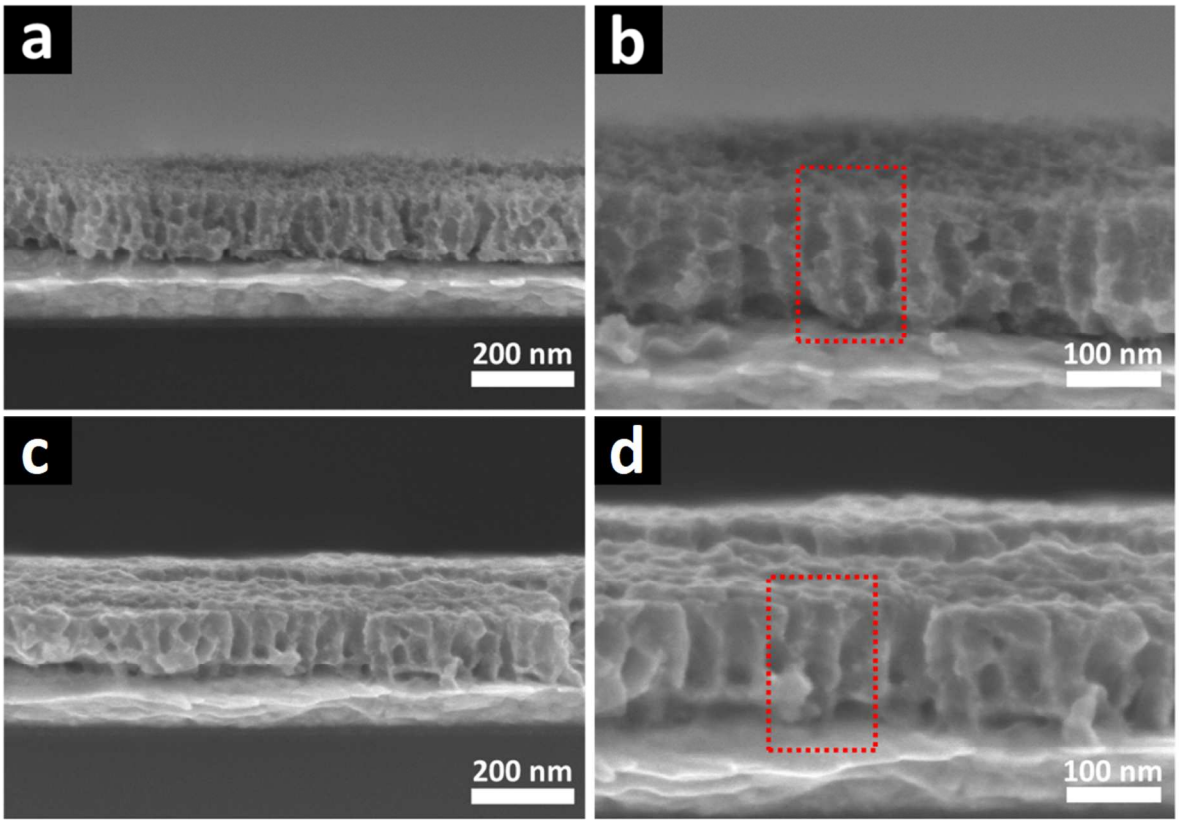

Figure S6 Cross-sectional SEM images of the mesoporous $Au_{78}Cu_{22}$ film (a) low- (b) high-magnification and the mesoporous $Au_{49}Cu_{51}$ film (c) low- (d) high-magnification.

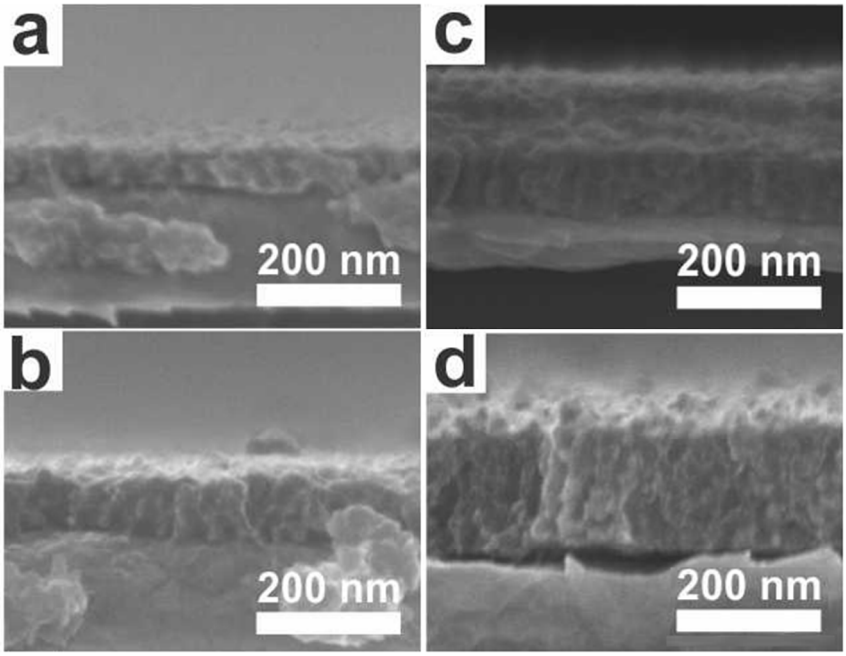

Figure S7 Cross-sectional SEM images of the mesostructured $Au_{49}Cu_{51}$ films with different reduction times before immersion in THF solution [(a) 500 s, (b) 750 s, (c) 1000 s, (d) 1750 s].

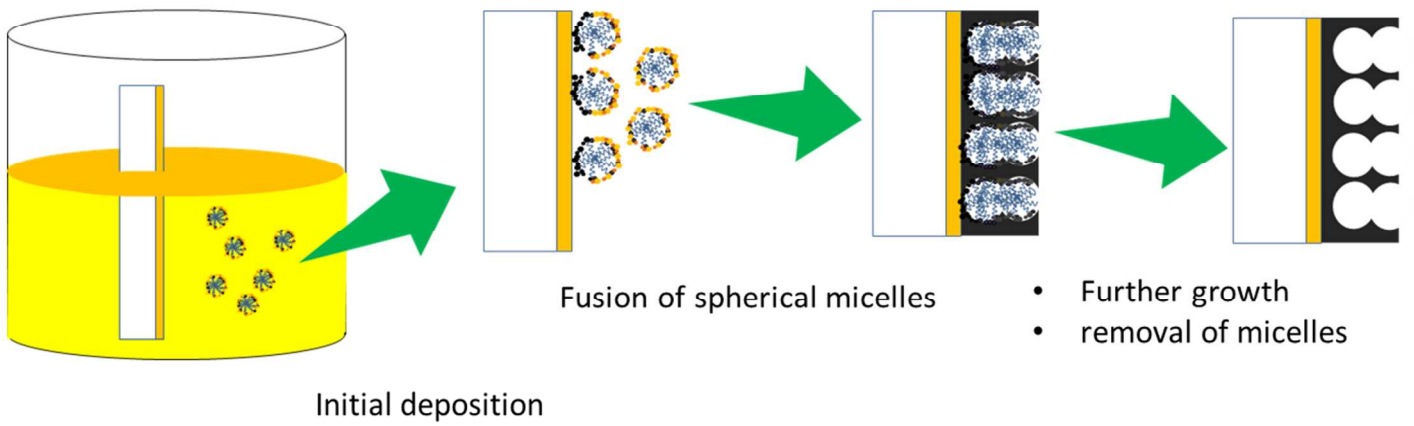

Figure S8 Schematic illustration of formation of vertically oriented mesochannels through the fusion of the spherical micelles.

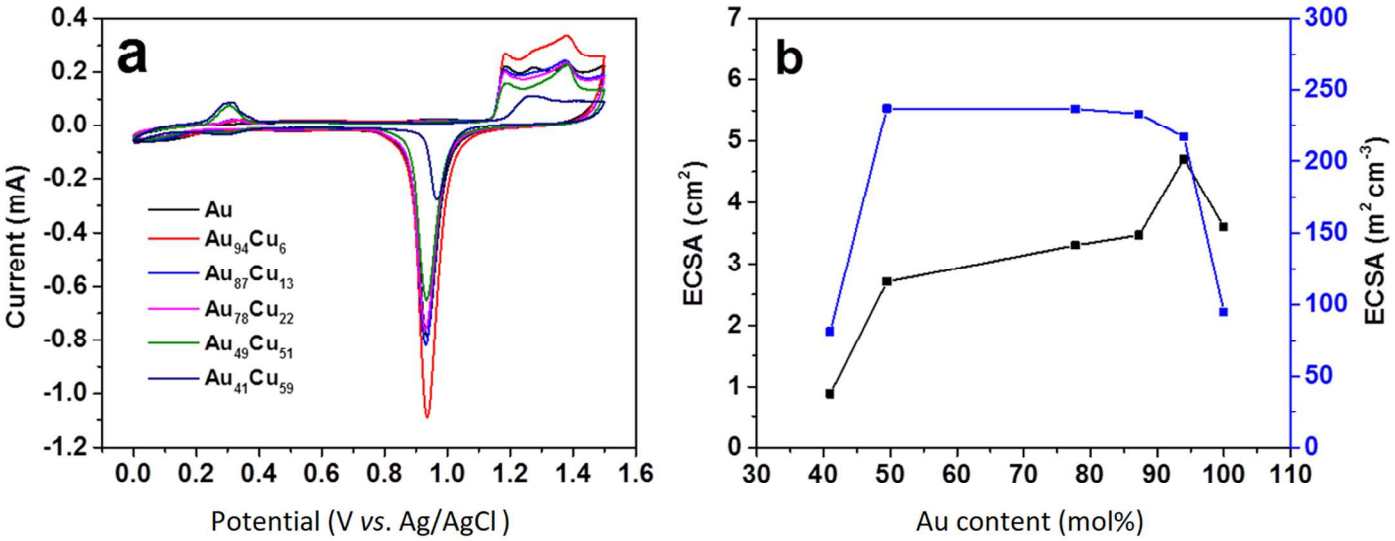

Figure S9 (a) CV measurements of the mesoporous Au-Cu films with different composition in 0.5 M H_2SO_4. (b) Relationship between the composition ratios, $ECSA_{(Au)}$ and volume-normalized $ECSA_{(Au)}$.

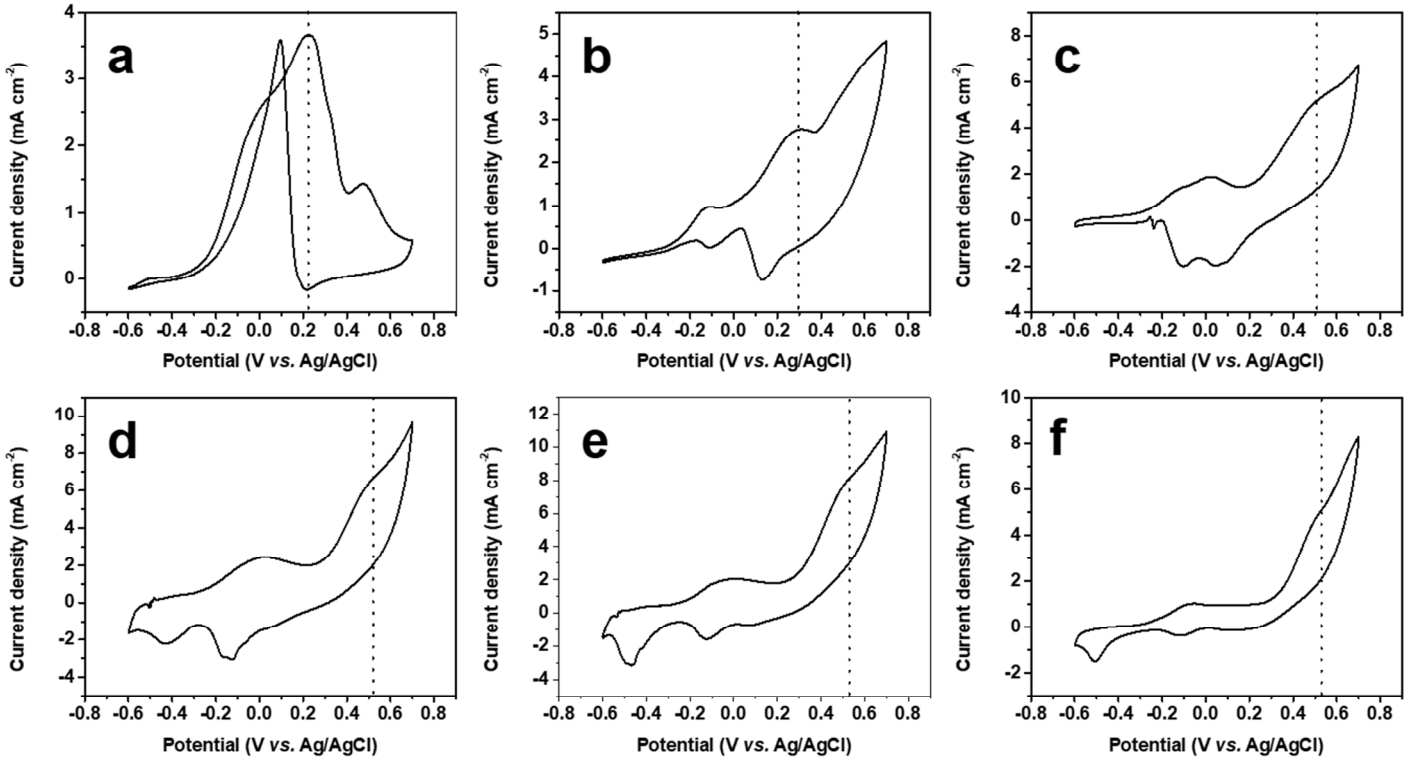

Figure S10 CVs of the mesoporous (a) Au_{100}, (b) $Au_{94}Cu_6$, (c) $Au_{87}Cu_{13}$, (d) $Au_{78}Cu_{22}$, (e) $Au_{49}Cu_{51}$, and (f) $Au_{41}Cu_{59}$ films. The current density was normalized by the geometrical electrode area. The glucose electro-oxidation peaks are highlighted by dot lines.

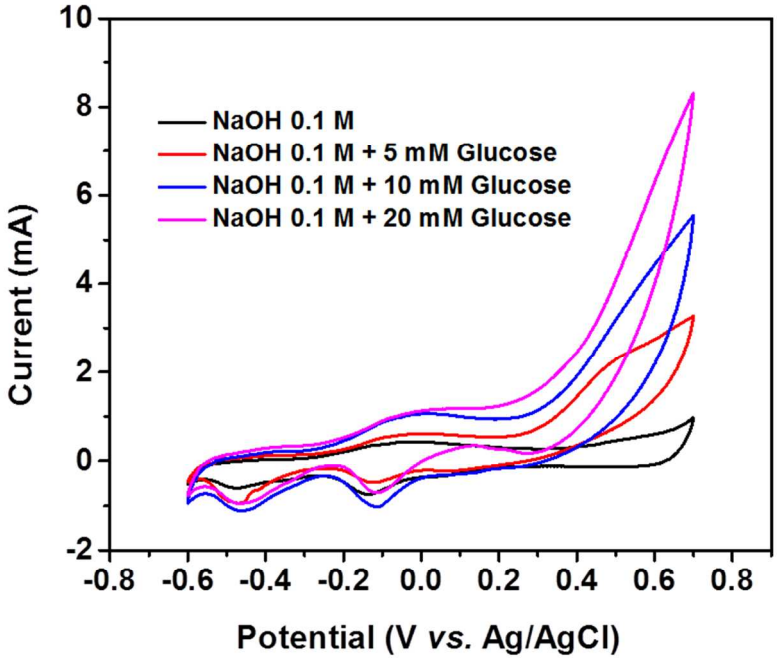

Figure S11 Cyclic voltammograms of the mesoporous $Au_{49}Cu_{51}$ in different concentrations of glucose. The scan rate is 50 mV s^{-1}.

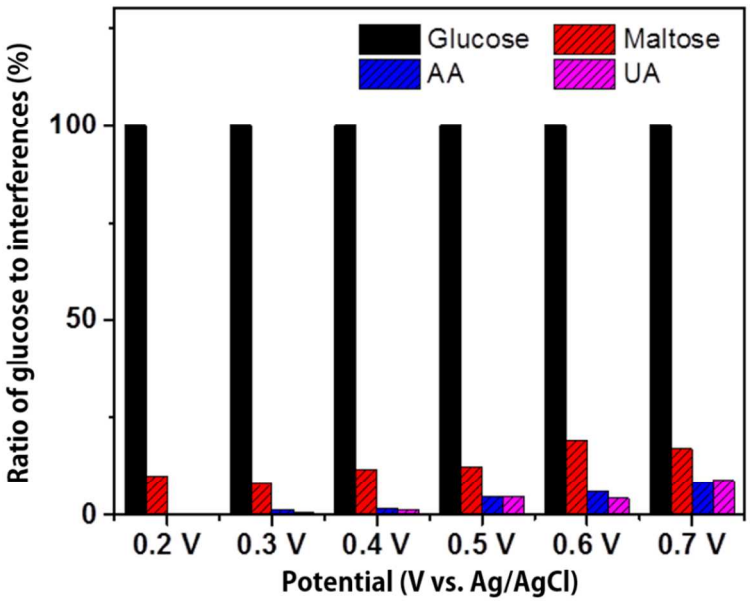

Figure S12 Effect of different applied potential on the amperometric response of mesoporous $Au_{49}Cu_{51}$ to glucose, ascorbic acid, uric acid, maltose in 0.1 M NaOH. The current density of glucose was taken as 100% and the current densities for interfering electroactive species were normalized by the current of glucose.

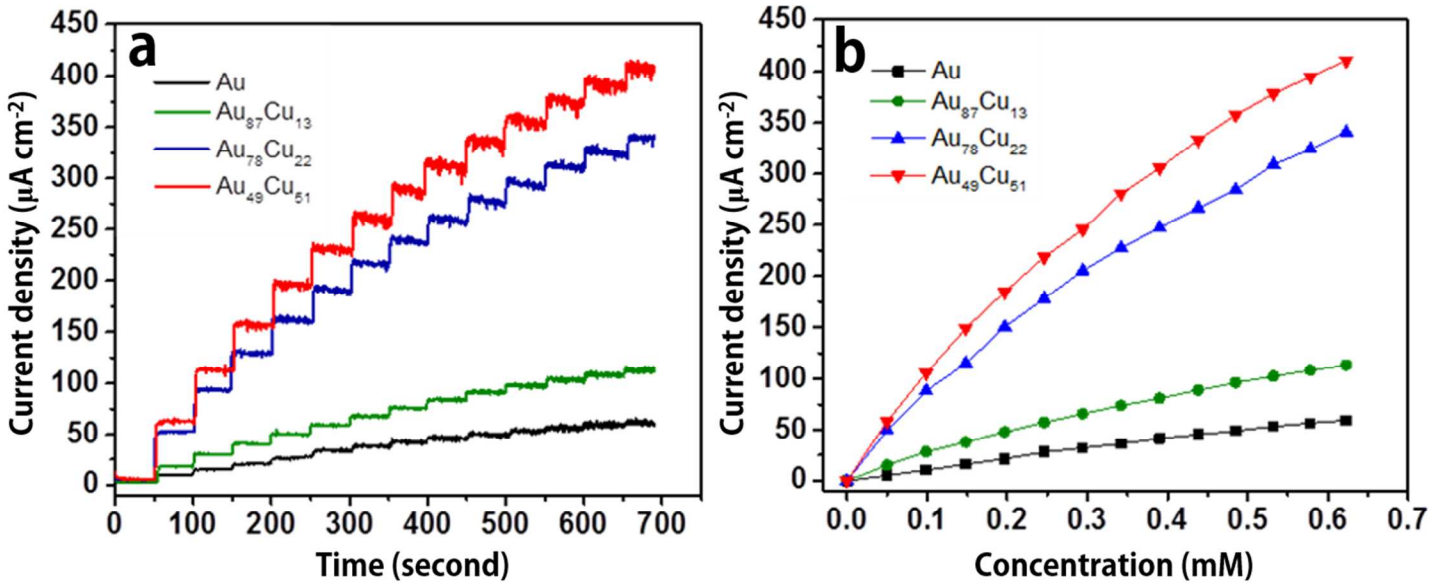

Figure S13 (a) Time dependent amperometry following successive the addition of glucose (0.05 mM) with the mesoporous films in 0.1 M NaOH at 0.3 V (*vs.* Ag/AgCl). (b) Corresponding calibration curves. The current response of the dynamic detection of glucose was normalized by the geometrical electrode area.

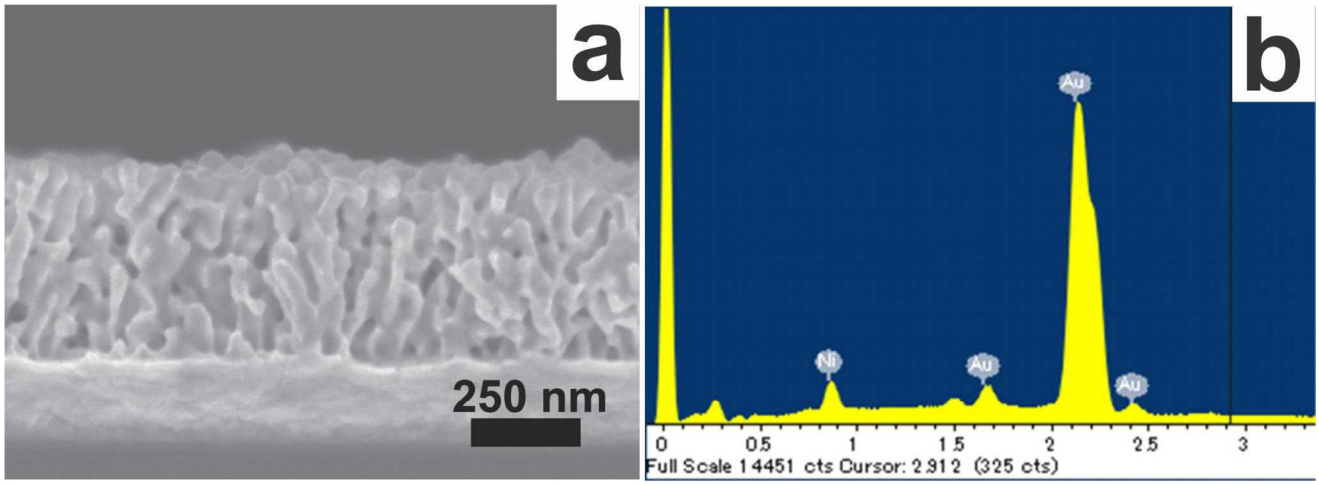

Figure S14 (a) Cross-sectional SEM images of the mesoporous Au-Ni film from the electrolyte solution with the compositional ratio of Au (75) : Ni (25). (b) Corresponding EDX spectra of the mesoporous Au-Ni film.